

Semantic Guidance Tuning for Text-To-Image Diffusion Models

Hyun Kang
Yonsei University
kdkh1125@yonsei.ac.kr

Dohae Lee
Yonsei University
dlehgo1414@yonsei.ac.kr

Myungjin Shin
Yonsei University
mjsh25@yonsei.ac.kr

In-Kwon Lee
Yonsei University
iklee@yonsei.ac.kr



Figure 1. ConceptDiffusion improves the text-to-image alignment by modulating the guidance of diffusion models towards any concept from which the model diverges. Our method follows text prompt faithfully compared to Stable Diffusion [35], which tends to neglect certain subject or incorrectly binds attributes. All images are generated using the same random seeds.

Abstract

Recent advancements in Text-to-Image (T2I) diffusion models have demonstrated impressive success in generating high-quality images with zero-shot generalization capabilities. Yet, current models struggle to closely adhere to prompt semantics, often misrepresenting or overlooking specific attributes. To address this, we propose a simple, training-free approach that modulates the guidance direction of diffusion models during inference. We first decompose the prompt semantics into a set of concepts, and monitor the guidance trajectory in relation to each concept. Our key observation is that deviations in model’s adherence to prompt semantics are highly correlated with divergence of the guidance

from one or more of these concepts. Based on this observation, we devise a technique to steer the guidance direction towards any concept from which the model diverges. Extensive experimentation validates that our method improves the semantic alignment of images generated by diffusion models in response to prompts.

1. Introduction

Text-to-Image (T2I) diffusion models [2, 8, 33–36] have taken significant strides recently in producing high-quality images from free-form text prompts with increasing diversity and visual fidelity. However, text-to-image synthesis

is still tempered by a key challenge: semantic misalignment between text prompts and generated images [4, 9, 45]. While diffusion models are adept at generating a single subject, they fail to faithfully adhere to the semantic subtleties of multi-subject text prompts [5, 7, 23]. The generated images often neglect one or more subjects in the prompt or incorrectly bind attributes between them as shown in Fig. 1.

Recent works have revealed that the diffusion process in latent diffusion models (*e.g.*, Stable Diffusion [35]) organizes high-level semantics and implicitly learns relationships between them without explicit supervision [3, 6, 46]. Such an understanding allows us to interpret the generation process of diffusion models as a reverse process: recomposing individual concepts into a cohesive scene. Therefore, any failure in accurately following the semantics of a scene suggests that one or more concepts may not be effectively reintegrated during this recomposition process. Figure 2 provides a visual representation of the guidance trajectory with respect to different concepts contained within the prompt. This visualization specifically highlights how the trajectory diverges from concepts that are neglected or inadequately represented in the model’s recomposition process.

In response, we propose a training-free approach to carefully modulate the guidance direction towards any concept from which the diffusion model diverges. Specifically, our method starts by extracting distinct concepts from the text prompt. We then measure the cosine similarity between the model’s score for the overall prompt and the score specific to each extracted concept. A lower cosine similarity is indicative of a concept potentially being neglected. Based on these similarity measurements, we adjust the guidance direction towards such concepts. Our experiments show that our method improves the diffusion models’ text-to-image alignment. We refer to our method as ConceptDiffusion.

Our contributions can be summarized as follows:

- We develop a technique to detect semantic misalignment of diffusion models during inference, enabling real-time correction.
- We propose an intuitive method to improve the alignment between text prompts and generated images, without requiring additional training or optimization.
- Through comprehensive and empirical evaluations, we demonstrate that ConceptDiffusion qualitatively and quantitatively improves the text-to-image alignment.

2. Related Works

Text-to-Image Models. In the initial exploration of the text-to-image synthesis task, GANs were at the forefront [39, 47, 48, 50, 52]. Subsequent advancements were marked by the advent of large-scale auto-regressive models, which demonstrated remarkable capabilities [33, 49]. The diffusion models [27, 34–36] recently have

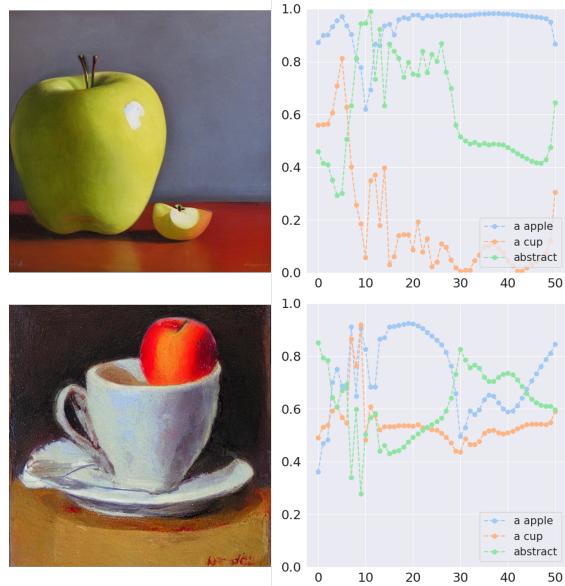


Figure 2. An illustration of images generated with a prompt “a cup and an apple” along with the similarity k of each concept plotted over timestep $t \in [0, T]$. When the model fails to synthesize “a cup”, the similarity k for the subject concept “a cup” diverges from the prompt score (top). Conversely, when the model successfully synthesizes both subjects, the similarity scores for each concept remain high and comparatively close (bottom).

emerged as a promising generative model with unparalleled photo-realism and stable training procedures. However, generated images by diffusion models often fail to closely adhere to the input prompt. To address this, classifier-free guidance [11] has been introduced to strengthen the prompt reliance, yet extensive prompt engineering is still required to achieve desired results [24]. Imagen [36], on the other hand, addresses the problem with improved text encoder model [32]. For our work, we focus on Stable Diffusion [35], the state-of-the-art open-sourced T2I model.

Semantic Dimensions. The concept of semantic dimensionality has been extensively explored in language models, where it is used to mirror semantic and linguistic relationships [25, 43]. A notable illustration of this is vector arithmetic within semantic dimensions, where an operation like ‘King – male + female’ yields a vector closely related to ‘Queen’. This characteristic enables meaningful interpolation of semantic vectors. For generative models, StyleGANs [14, 15] have demonstrated the presence of semantic dimensions that can be leveraged during image generation. In the context of diffusion models, several works have uncovered semantic latent spaces within frozen pre-trained diffusion models [3, 19]. Concurrent studies revealed the meaningful interpretation of concept represen-

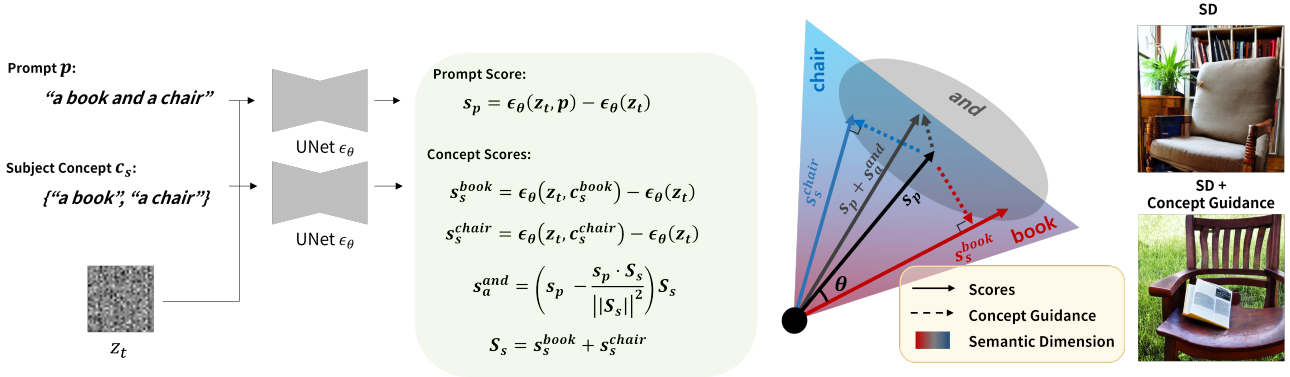


Figure 3. **Overview of ConceptDiffusion.** Given a prompt *e.g.* “a book and a chair”, we extract the subject concepts {“a book”, “a chair”} and compute their corresponding scores. The score for abstract concept “and” is indirectly obtained. The Concept Guidance is then applied based on the cosine similarity between the prompt score and score for each concept.

tations within these semantic spaces. [6, 46]. Building upon these findings, our work utilizes the semantic dimension in pre-trained diffusion models to adjust the guidance vector towards the inclusion of concepts that are otherwise missing in the generation process.

Controllable Image Synthesis. For a more controllable generation, recent works have proposed methods to synthesize images with additional spatial control [1, 8, 20, 26, 42, 44, 51]. Another line of works explores providing users control solely through text [4, 16, 40]. While these models provide not only a layer of control over the image generation process but also tend to adhere more closely to input prompts, they require extra inputs from users. Moreover, these methods may require fine-tuning of pre-trained models [1] or the integration of new modules like adapters [20, 26, 51]. For more precise control, several works have proposed methods to edit the image in diffusion models’ latent space [3, 9, 46]. Our work aligns with these developments and can be viewed as a one-shot generation method that edits an image on-the-fly to encapsulate the input prompt semantics in its entirety.

Compositional Generation. Another line of works tries to address the misalignment between input prompts and generated images using training-free methods. Composable Diffusion [23] employs separate denoising processes for distinct phrases derived from the input prompt, leveraging the score-based interpretation of diffusion models. The noise-estimates for each phrase are added to attain a unified image. This method combines noise estimates from each phrase to create a unified image. Structure Diffusion [7] takes a different approach by modulating cross-attention maps based on consistency trees or scene graphs derived from the input prompt. Similarly, Attend-and-Excite [5]

aims to enhance the representation of overlooked tokens in cross-attention maps through explicit gradient-based optimization of noise estimates. Our work Concept Diffusion is closely related to the Composable Diffusion in its fundamental approach of manipulating the noise-estimates of diffusion models without training and optimization.

3. Method

3.1. Latent Diffusion Models

We apply our method and experiment on the state-of-the-art T2I model, Stable Diffusion (SD) [35]. SD consists of two modules, an auto-encoder and a diffusion model. An encoder \mathcal{E} is trained to map a given image x in RGB space to a latent space, $z = \mathcal{E}(x)$. A decoder \mathcal{D} is to reconstruct the image from the latent, such that $\tilde{x} = \mathcal{D}(z) = \mathcal{D}(\mathcal{E}(x))$.

Operating on the learned latent space of the autoencoder, the denoising diffusion probabilistic model (DDPM) [12, 37] gradually denoises an input latent vector z_t at each timestep t into a less noisy vector z_{t-1} . During the denoising process, the diffusion model is conditioned on an input prompt p , which is encoded by a pre-trained CLIP text encoder [30]. The DDPM model ϵ_θ is trained with objective,

$$\mathbb{E}_{z \sim \mathcal{E}(x), p, \epsilon \sim \mathcal{N}(0, I), t} \left[\|\epsilon - \epsilon_\theta(z_t, t, p)\|_2^2 \right], \quad (1)$$

where t is drawn from uniform distribution $t \sim \mathcal{U}([0, 1])$ and ϵ is sampled from a Gaussian distribution $\epsilon \sim \mathcal{N}(0, I)$. The model is trained to denoise z_t by estimating the noise ϵ added to the latent vector at each timestep t .

Classifier-free guidance [11] is a conditioning method that does not require an additional pre-trained classifier by intermittently omitting the text conditioning at a predetermined probability. This process results in fulfilling both unconditional and conditional objectives. During inference,

the noise estimate of the diffusion models are adjusted as

$$\epsilon_\theta(z_t, t, p) = \epsilon_\theta(z_t, t) + w_g \left(\epsilon_\theta(z_t, t, p) - \epsilon_\theta(z_t, t) \right), \quad (2)$$

in which w_g is the guidance scale.

The noise estimate can be interpreted as the score of an underlying unnormalized Energy-Based Model [23, 38, 41]. This interpretation enables us to consider the noise estimate for prompt condition $\epsilon_\theta(z_t, t, p)$ as a composite of concepts $\mathcal{C} = \{c_1, c_2, \dots, c_n\}$ that can be expressed as,

$$\epsilon_\theta(z_t, t, p) = \epsilon_\theta(z_t, t) + \sum_{i=1}^n w_i \left(\epsilon_\theta(z_t, t, c_i) - \epsilon_\theta(z_t, t) \right), \quad (3)$$

in which w_i represents the weighting factor for each concept.

3.2. Concept Diffusion

Our goal is to regulate the noise estimate of diffusion models at each timestep t to achieve improved semantic alignment between the prompt and the generated image, without fine-tuning or optimization. We hypothesize that the cause of semantic misalignment is correlated to the divergence of the noise estimate from one or more concepts that are critical for successful synthesis. In Fig. 3, we show a framework of our proposed method.

Concept Extraction To address this, we first define the ideal concepts that should be represented in the noise estimate. Intuitively, in order for a subject to be present in the image, the noise estimate must contain semantics of it as well. Therefore, given a prompt p , we extract all the individual subjects (*i.e.*, noun phrases). These are referred to as subject concepts, denoted by $C_s = \{c_s^1, c_s^2, \dots, c_s^n\}$, where n represents the total number of subjects. We leave the rest of the concepts present in the noise estimate unknown and collectively refer them to an abstract concept c_a . Now, rewriting Eq. (3) in terms of the concepts we defined gives,

$$\epsilon_\theta(z_t, t, p) = \epsilon_\theta(z_t, t) + \sum_{i=1}^n w_s^i \left(\epsilon_\theta(z_t, t, c_s^i) - \epsilon_\theta(z_t, t) \right) + w_a \left(\epsilon_\theta(z_t, t, c_a) - \epsilon_\theta(z_t, t) \right), \quad (4)$$

where w_s^i and w_a represent weighting factors for each concept.

Weight Measurement In this context, the inclusion of a concept in the noise estimate is indicated by its respective weighting factor. When the weight assigned to a particular concept drops significantly, it suggests a decreased likelihood of that concept being represented in the generated

image. We define such notable reductions in a concept’s weighting factor, especially when compared to other factors that remain stable, as a divergence. Therefore, we suppose a divergence as a key indicator of how closely each concept is represented in the noise estimate, guiding us in adjusting the model for better semantic alignment. However, the noise estimate of diffusion models is high dimensional that it is not feasible to disentangle the noise estimate into an arbitrary set of concepts that we defined. Consequently, the exact numerical values of the weighting factors of the concepts cannot be calculated. We thus propose an indirect method to approximate the scale of each concept we defined. To do so, we first perform forward passes through the diffusion model with p and C_s separately to obtain scores s_p and s_s^i for each using the same latent z_t :

$$\begin{aligned} s_p &= \epsilon_\theta(z_t, t, p) - \epsilon_\theta(z_t, t), \\ s_s^i &= \epsilon_\theta(z_t, t, c_s^i) - \epsilon_\theta(z_t, t), \quad i \in [1, n]. \end{aligned} \quad (5)$$

The scores represent the direction in which the prompt p and each subject concept c_s^i influence the noise estimate. Specifically, the scores for the subject concepts represent their respective influences within the overall prompt score s_p , thus providing insights into how each concept contributes to the direction of the noise estimate.

Given that the abstract concept represents the negation of subject concepts, the score s_a of abstract concept can be calculated through an orthogonal projection,

$$s_a = s_p - \frac{s_p \cdot S_s}{\|S_s\|^2} S_s, \quad \text{where } S_s = \sum_{i=1}^n s_s^i. \quad (6)$$

This method ensures s_a to capture the overall structural composition of the image, as opposed to the specific elements depicted by the subject concepts. Consider the prompt ‘‘a cat and a dog’’. In this case, the abstract concept, derived from the negation of the subject concepts ‘a cat’ and ‘a dog’, conveys the spatial or relational interaction between these subjects – the coexistence of two objects, in this case. Fig. 4 demonstrates the images generated using the scores of each individual concept. Notably, the image created based on the abstract concept score exhibits alignment with the overall structural composition of the image generated using the prompt score. This alignment illustrates the efficacy of our method in isolating and emphasizing each concept, particularly in capturing the broader, abstract relationships and structures implied by the prompt.

Now that we have defined the score of concepts that constitute the prompt score s_p , we measure the cosine similarity, denoted as k , between the score derived from the prompt s_p and the score for each concept $s_c \in \{s_a, s_s^1, s_s^2, \dots, s_s^n\}$ as a proxy to measure the weighting factor associated with each concept. The cosine similarity $k(s_p, s_c)$ between s_p



Figure 4. An illustration of images generated using the prompt score and concept scores with the prompt “a cat and a dog”. The images highlight how the abstract concept score aligns with the overall structural composition of the prompt, demonstrating the ability of our method to isolate and emphasize both specific subjects and their relationship.

and s_c is denoted as

$$k(s_p, s_c) = \left| \frac{s_p \cdot s_c}{\|s_p\| \|s_c\|} \right|. \quad (7)$$

A high degree of cosine similarity indicates a semantic overlap of the prompt score and the concept score. Consequently, this suggests a high weighting scale of the concept.

Our key finding is that these similarity measurements are strongly correlated with the degree of semantic alignment in the generated images. Fig. 2 graphically demonstrates this relationship, showing the cosine similarity k of each concept across timesteps $t \in [0, T]$. In scenarios where the model accurately synthesizes all subjects in the prompt, we observe that the similarity scores for each concept are consistently high and closely aligned. Meanwhile, when the model fails to accurately render a specific concept, the similarity score for that concept fluctuates and generally remains lower, highlighting the direct impact of concept representation on the quality of the generated image.

Concept Guidance Based on the observation that the cosine similarity k is associated with semantic alignment, we propose a concept guidance term ϕ that modulates the noise estimate of the diffusion model based on the similarity. Formally, extended to Eq. (2), we compute,

$$\epsilon_{\theta}(z_t) + w_g s_p + \phi(z_t, S_c, s_p), \quad (8)$$

in which $S_c = \{s_a, s_s^1, s_s^2, \dots, s_s^n\}$. The concept guidance ϕ

is defined as,

$$\phi(z_t, S_c, s_p) = w_c \sum \gamma(s_p, s_c, \eta) \psi(s_c, s_p), \quad (9)$$

where w_c is the concept guidance scale and $s_c \in S_c$. The γ is a delta function based on the cosine similarity between s_p and s_c ,

$$\gamma(s_p, s_c, \eta) = \begin{cases} 1, & k(s_c, s_p) < \eta \\ 0, & \text{otherwise.} \end{cases} \quad (10)$$

The threshold η is a hyperparameter that corresponds to the minimum inclusion of a concept in prompt score. Naturally, larger η increases the effect of concept guidance. We empirically found that $\eta = 1/(n+1)$ generally works well. The guidance direction $\psi(s_p, s_c)$ is determined as,

$$\psi(s_p, s_c) = \begin{cases} s_c - \frac{s_c \cdot s_p}{\|s_c\|^2}, & \text{if subject concept} \\ s_c, & \text{if abstract concept.} \end{cases} \quad (11)$$

For subject concepts, a lower cosine similarity suggests a divergence of it from the prompt score. In such cases, our approach involves steering the model’s guidance towards these concepts to ensure their inclusion. Conversely, the abstract concept is understood as an independent component of the main score that is distinct from the subject concepts. Therefore, a low cosine similarity here indicates that the main score closely resembles the aggregate of subject concepts, potentially leading to a fusion of concepts in the generated results. To counteract this, when the cosine similarity for the abstract concept decreases, we adjust the guidance so that $k(s_p, \sum s_s) > \eta$.

Note that our method doesn’t need extra training or optimization and can be used with any diffusion model that uses classifier-free guidance [11].

4. Experiments

4.1. Experiments Setting

Baselines. We compare our method with various *training-free* methods, namely Composable Diffusion [23], Structure Diffusion [7], and Attend-and-Excite [5], along with Stable Diffusion [35]. Since Composable Diffusion requires the input prompt to follow the pattern of noun phrases joined together by conjunction *and* or *not*, we deconstruct each prompt into its constituent noun phrases and subsequently reassemble them using a conjunction *and*. We use constituency trees for language parser in Structure Diffusion. For Attend-and-Excite, all nouns present in the prompt are *excited* by the model.

Metrics. We evaluate each method on the image quality and the alignment of the input prompt and the generated

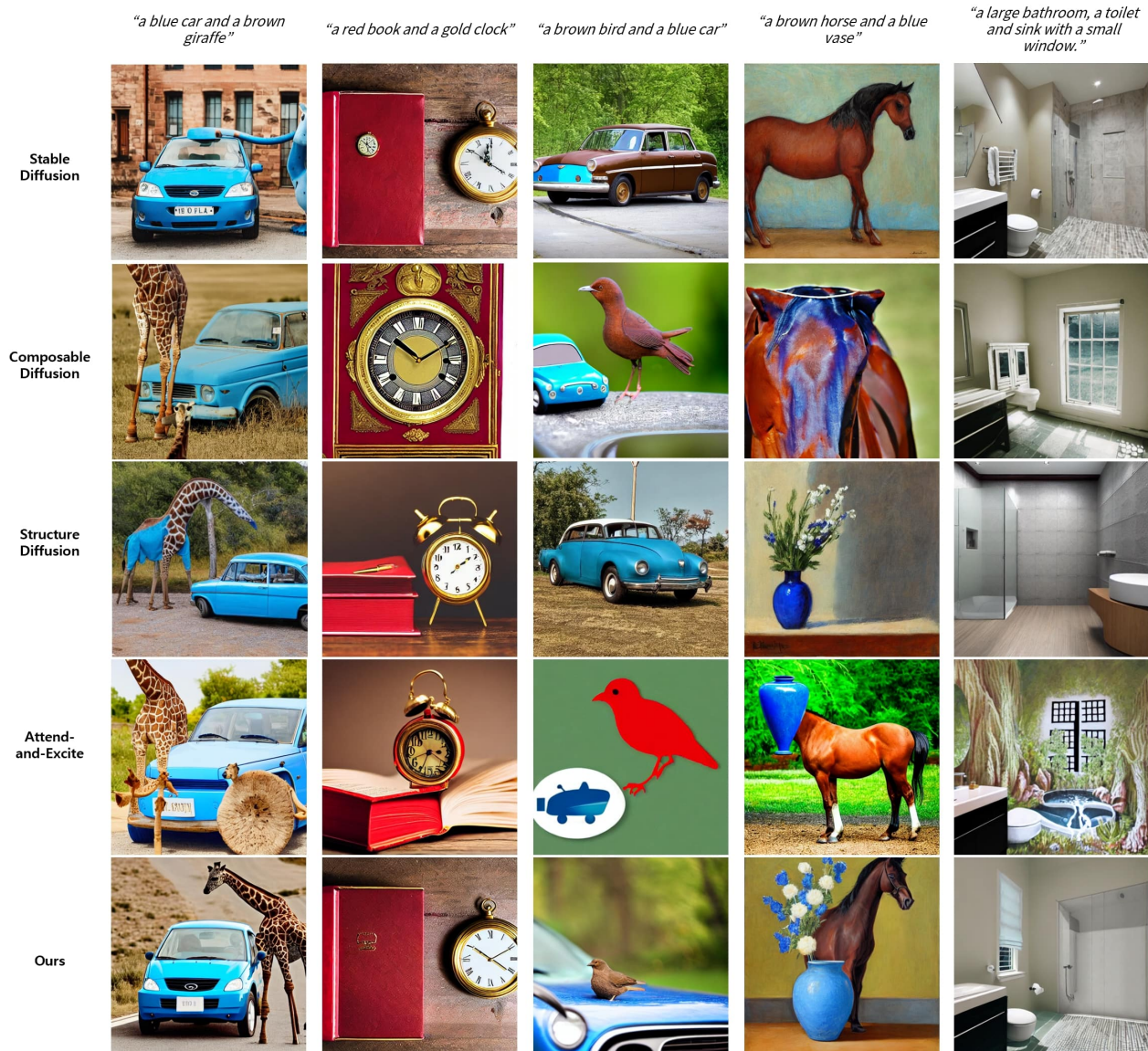


Figure 5. **Qualitative Results.** Comparison to baseline methods on CC-500 dataset [7]. All images are generated using same random seed.

	CC-500			Dense MS-COCO		
	FID↓	R-Prec.↑	BLIP-VQA↑	FID↓	R-Prec.↑	BLIP-VQA↑
Stable Diffusion	75.62	0.318	0.294	71.4	0.320	0.458
Composable Diffusion	77.53	0.315	0.351	63.0	0.297	0.304
Structure Diffusion	81.71	0.312	0.299	68.8	0.314	0.432
Attend-and-Excite	71.44	<u>0.329</u>	0.537	72.3	<u>0.324</u>	0.539
Ours	<u>72.91</u>	0.334	<u>0.485</u>	<u>65.2</u>	0.327	<u>0.509</u>

Table 1. **Quantitative Results.** FID reflects the quality of images generated. CLIP R-Precision (R-Prec.) and BLIP-VQA evaluates the semantic alignment between the prompts and corresponding images. the best-performing metrics are highlighted in **bold**, while the second-best results are underlined. Our method is generally on par with the State-of-the-Art method Attend-and-Excite.

image. To measure the fidelity of the image generated, we follow previous works to utilize Fréchet Inception Distance

(FID) [10], which is the distance between feature vectors calculated for real and generated images. For text-to-image

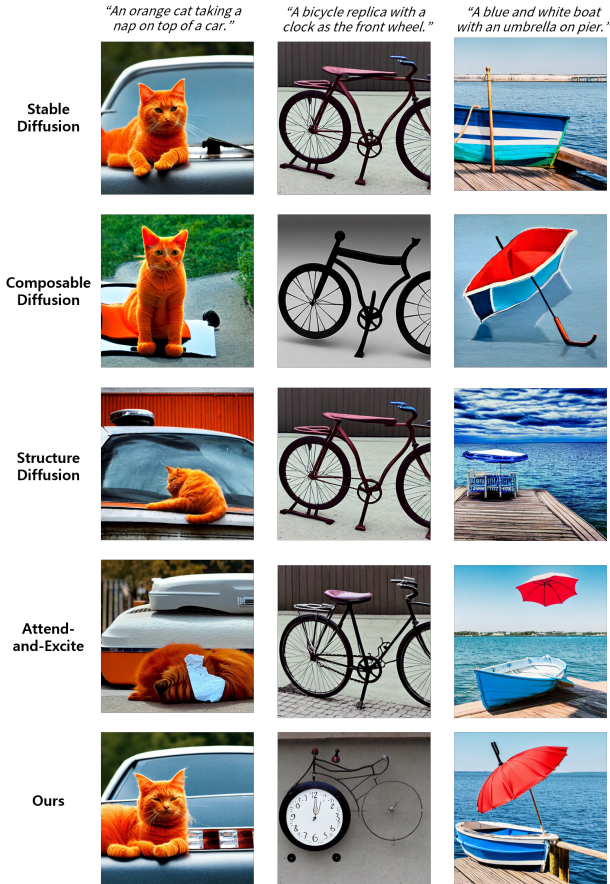


Figure 6. More comparison on Dense MS-COCO dataset [7].

alignment we measure CLIP R-precision (R-prec.) [28] that measures how precisely a model can retrieve a relevant image from a set of images given a text prompt. However, since it is reported in failing to measure fine-grained correspondences such as attribute binding [31, 36]. We utilize BLIP-VQA [13] for attribute binding evaluation. Lastly, we conduct a human evaluation on both image fidelity and image-text alignment as in [18].

Datasets. We use Concept Conjunction 500 (CC-500) dataset [7], which is consisted of prompts that conjunct multiple subjects together. We also evaluate on Dense MS-COCO [17] to measure the generalization capability of each method on more complex prompts.

4.2. Results

Qualitative Analysis. In Fig. 5, we present a comparative analysis of ConceptDiffusion against various baseline methods, using images generated from the CC-500 dataset [7] with same random seeds. This comparison clearly illustrates that our method, ConceptDiffusion, achieves improved semantic alignment between the input prompts and

the generated images. Although all the other baseline methods generally improve the performance as well, there are some notable drawbacks for each. For instance, Composable Diffusion [23] often blends subjects from the prompt in a literal sense. An example of this is seen with the prompt, “a red book and a gold clock”, it generates a red book with an embedded gold clock. Similarly, it generates a horse with vase-like head for the prompt “a brown horse and a blue vase”. Structure Diffusion [7], on the other hand, struggles to generate all the subjects or correctly bind attributes when the images generated by Stable Diffusion are substantially different from the input prompt. For Attend-and-Excite [5], although the method mostly generate all the subjects in the prompt, it tends to turn the images into paintings as can be seen in the third and fifth column. Furthermore, the arrangement of subjects sometimes appears unrealistic, such as a floating vase in the image for the prompt “a brown horse and a blue vase”. ConceptDiffusion, in comparison, not only accurately synthesizes all subjects from the prompt but also ensures their natural composition within the image. For example, for the prompt “a brown bird and a blue car”, our method produces an image of a bird perched on a car, which is a more realistic composition compared compared to that of Composable Diffusion. In addition, when the images generated by Stable Diffusion closely aligns with the prompt’s semantics, as in the case of the prompt “a red book and a gold clock”, our method applies minimal modifications, preserving the core elements of the image. Conversely, ConceptDiffusion demonstrates its robustness in scenarios where the generated images of Stable Diffusion deviate significantly from the intended semantics of the prompt. For instance, with prompts like “a brown horse and a blue vase”, ConceptDiffusion makes more extensive structural adjustments. This adaptability suggests the method’s ability to tailor its modifications according to the degree of semantic misalignment.

Fig. 6 further demonstrates the capability of baseline methods on more complex prompts. Many baseline models struggle to accurately represent prompts that involve intricate relationships between subjects or specific state. For the prompt “an orange cat taking a nap on top of a car”, several baseline methods successfully generate images that include all the subjects, yet they fall short in depicting the spatial relationship “on top” or the state of the cat “taking a nap”. In contrast, Concept Diffusion outperforms in reflecting these relationships and the states.

Quantitative Analysis. In Tab. 1, we quantify the performance of each method based on the quality of images generated and the text-to-image alignment.

To evaluate the quality of images generated by each method, we randomly select 6 and 10 seeds to generate images, amounting to 3000-5000 images for CC-500 dataset

	CC-500		Dense COCO	
	PQ	SC	PQ	SC
Stable Diffusion	18.3	5.0	23.3	3.3
Composable Diffusion	3.3	1.7	1.7	0
Structure Diffusion	15.0	6.7	6.7	0
Attend-and-Excite	26.7	36.7	28.3	33.3
Ours	36.7	50.0	40.0	63.3

Table 2. We generate an image for 20 randomly selected prompts for each dataset. Users are asked to select one with best quality (PQ) and one that follows the prompt best (SC). The result shows the percentage of preference.

and Dense MS-COCO dataset, respectively. We then measure the FID against the MS-COCO 2017 validation dataset [21]. Our analysis revealed that baseline methods tend to degrade the quality of the generated images, as indicated by an increase in FID scores. Notably, Concept Diffusion improves the quality of images generated on both datasets.

The results from our text-to-image alignment evaluations clearly demonstrate that Concept Diffusion significantly enhances the semantic alignment between text prompts and the corresponding generated images. In terms of R-Precision scores, which measures the similarity of image feature and text feature in pre-trained model, our method outperforms the baseline models, achieving a substantial increase compared to Stable Diffusion. Additionally, when evaluated using BLIP-VQA, our method shows performance that is on par with Attend-and-Excite, although our method does not require explicit gradient-based optimization during inference.

We further evaluate the semantic alignment with a user study. For each prompt, we generated images using the same random seed across different methods. Participants are asked to select the image they consider to have the best quality and the one that most closely followed the prompt. Tab. 2 shows that users prefer our method over baseline methods especially on complex Dense MS-COCO dataset, despite lower BLIP-VQA score. This outcome suggests that Concept Diffusion potentially improves the performance in capturing the broader semantics of the prompt as BLIP-VQA primarily assesses attribute binding.

5. Conclusion

In this work, we introduce a novel approach designed to enhance the text-to-image synthesis process in diffusion models, notably without the need for fine-tuning or optimization. Our key finding is that semantic misalignment in the synthesis process can be effectively identified on-the-fly. This is achieved by measuring the cosine similarity between the noise estimate and the scores of the concepts extracted from the text prompt. Through



Figure 7. **Limitations.** An attribute for subjects are bound to background (left); The subject combination results in fusion (middle); An initially presented subject disappear (right).

extensive experimentation, we demonstrate that Concept Diffusion significantly improves text-to-image alignment, with capability to capture complex semantics such as relationship between subjects. This advancement underscores the effectiveness of our method in generating contextually coherent and visually accurate images from descriptive prompts.

Limitations. Our method has several limitations as illustrated in Fig. 7. First, our method often binds attributes of a subject to background as shown in the left. This is inherited from Stable Diffusion, which captures entangled semantics. Second, there are cases in which the model results in fusion or swapping of subjects as an example in the middle and right. Future work may explore the isolation of attributes for more precise control of noise estimate.

References

- [1] Omri Avrahami, Thomas Hayes, Oran Gafni, Sonal Gupta, Yaniv Taigman, Devi Parikh, Dani Lischinski, Ohad Fried, and Xi Yin. Spatext: Spatio-textual representation for controllable image generation. In *Proceedings of the IEEE/CVF Conference on Computer Vision and Pattern Recognition*, pages 18370–18380, 2023. 3
- [2] Yogesh Balaji, Seungjun Nah, Xun Huang, Arash Vahdat, Jiaming Song, Karsten Kreis, Miika Aittala, Timo Aila, Samuli Laine, Bryan Catanzaro, et al. ediffi: Text-to-image diffusion models with an ensemble of expert denoisers. *arXiv preprint arXiv:2211.01324*, 2022. 1, 2
- [3] Manuel Brack, Felix Friedrich, Dominik Hintersdorf, Lukas Struppek, Patrick Schramowski, and Kristian Kersting. Sega: Instructing diffusion using semantic dimensions. *arXiv preprint arXiv:2301.12247*, 2023. 2, 3
- [4] Tim Brooks, Aleksander Holynski, and Alexei A Efros. Instructpix2pix: Learning to follow image editing instructions. In *Proceedings of the IEEE/CVF Conference on Computer Vision and Pattern Recognition*, pages 18392–18402, 2023. 2, 3
- [5] Hila Chefer, Yuval Alaluf, Yael Vinker, Lior Wolf, and Daniel Cohen-Or. Attend-and-excite: Attention-based semantic guidance for text-to-image diffusion models. *ACM Transactions on Graphics (TOG)*, 42(4):1–10, 2023. 2, 3, 5, 7

- [6] Hila Chefer, Oran Lang, Mor Geva, Volodymyr Polosukhin, Assaf Shocher, Michal Irani, Inbar Mosseri, and Lior Wolf. The hidden language of diffusion models. *arXiv preprint arXiv:2306.00966*, 2023. 2, 3
- [7] Weixi Feng, Xuehai He, Tsu-Jui Fu, Varun Jampani, Arjun Akula, Pradyumna Narayana, Sugato Basu, Xin Eric Wang, and William Yang Wang. Training-free structured diffusion guidance for compositional text-to-image synthesis. *arXiv preprint arXiv:2212.05032*, 2022. 2, 3, 5, 6, 7
- [8] Oran Gafni, Adam Polyak, Oron Ashual, Shelly Sheynin, Devi Parikh, and Yaniv Taigman. Make-a-scene: Scene-based text-to-image generation with human priors. In *European Conference on Computer Vision*, pages 89–106. Springer, 2022. 1, 3
- [9] Amir Hertz, Ron Mokady, Jay Tenenbaum, Kfir Aberman, Yael Pritch, and Daniel Cohen-Or. Prompt-to-prompt image editing with cross attention control. *arXiv preprint arXiv:2208.01626*, 2022. 2, 3
- [10] Martin Heusel, Hubert Ramsauer, Thomas Unterthiner, Bernhard Nessler, and Sepp Hochreiter. Gans trained by a two time-scale update rule converge to a local nash equilibrium. *Advances in neural information processing systems*, 30, 2017. 6
- [11] Jonathan Ho and Tim Salimans. Classifier-free diffusion guidance. *arXiv preprint arXiv:2207.12598*, 2022. 2, 3, 5
- [12] Jonathan Ho, Ajay Jain, and Pieter Abbeel. Denoising diffusion probabilistic models. *Advances in neural information processing systems*, 33:6840–6851, 2020. 3
- [13] Kaiyi Huang, Kaiyue Sun, Enze Xie, Zhenguo Li, and Xihui Liu. T2i-compbench: A comprehensive benchmark for open-world compositional text-to-image generation. *arXiv preprint arXiv:2307.06350*, 2023. 7
- [14] Tero Karras, Samuli Laine, and Timo Aila. A style-based generator architecture for generative adversarial networks. In *Proceedings of the IEEE/CVF conference on computer vision and pattern recognition*, pages 4401–4410, 2019. 2
- [15] Tero Karras, Samuli Laine, Miika Aittala, Janne Hellsten, Jaakko Lehtinen, and Timo Aila. Analyzing and improving the image quality of stylegan. In *Proceedings of the IEEE/CVF conference on computer vision and pattern recognition*, pages 8110–8119, 2020. 2
- [16] Bahjat Kawar, Shiran Zada, Oran Lang, Omer Tov, Huiwen Chang, Tali Dekel, Inbar Mosseri, and Michal Irani. Imagic: Text-based real image editing with diffusion models. In *Proceedings of the IEEE/CVF Conference on Computer Vision and Pattern Recognition*, pages 6007–6017, 2023. 3
- [17] Yunji Kim, Jiyoung Lee, Jin-Hwa Kim, Jung-Woo Ha, and Jun-Yan Zhu. Dense text-to-image generation with attention modulation. In *Proceedings of the IEEE/CVF International Conference on Computer Vision*, pages 7701–7711, 2023. 7, 1, 4
- [18] Max Ku, Tianle Li, Kai Zhang, Yujie Lu, Xingyu Fu, Wenwen Zhuang, and Wenhui Chen. Imagenhub: Standardizing the evaluation of conditional image generation models. *arXiv preprint arXiv:2310.01596*, 2023. 7
- [19] Mingi Kwon, Jaeseok Jeong, and Youngjung Uh. Diffusion models already have a semantic latent space. *arXiv preprint arXiv:2210.10960*, 2022. 2
- [20] Yuheng Li, Haotian Liu, Qingyang Wu, Fangzhou Mu, Jianwei Yang, Jianfeng Gao, Chunyuan Li, and Yong Jae Lee. Gligen: Open-set grounded text-to-image generation. In *Proceedings of the IEEE/CVF Conference on Computer Vision and Pattern Recognition*, pages 22511–22521, 2023. 3
- [21] Tsung-Yi Lin, Michael Maire, Serge Belongie, Lubomir Bourdev, Ross Girshick, James Hays, Pietro Perona, Deva Ramanan, C. Lawrence Zitnick, and Piotr Dollár. Microsoft coco: Common objects in context, 2015. 8
- [22] Luping Liu, Yi Ren, Zhijie Lin, and Zhou Zhao. Pseudo numerical methods for diffusion models on manifolds. *arXiv preprint arXiv:2202.09778*, 2022. 1
- [23] Nan Liu, Shuang Li, Yilun Du, Antonio Torralba, and Joshua B Tenenbaum. Compositional visual generation with composable diffusion models. In *European Conference on Computer Vision*, pages 423–439. Springer, 2022. 2, 3, 4, 5, 7
- [24] Vivian Liu and Lydia B Chilton. Design guidelines for prompt engineering text-to-image generative models. In *Proceedings of the 2022 CHI Conference on Human Factors in Computing Systems*, pages 1–23, 2022. 2
- [25] Tomas Mikolov, Kai Chen, Greg Corrado, and Jeffrey Dean. Efficient estimation of word representations in vector space. *arXiv preprint arXiv:1301.3781*, 2013. 2
- [26] Chong Mou, Xintao Wang, Liangbin Xie, Jian Zhang, Zhongqiang Qi, Ying Shan, and Xiaohu Qie. T2i-adapter: Learning adapters to dig out more controllable ability for text-to-image diffusion models. *arXiv preprint arXiv:2302.08453*, 2023. 3
- [27] Alex Nichol, Prafulla Dhariwal, Aditya Ramesh, Pranav Shyam, Pamela Mishkin, Bob McGrew, Ilya Sutskever, and Mark Chen. Glide: Towards photorealistic image generation and editing with text-guided diffusion models. *arXiv preprint arXiv:2112.10741*, 2021. 2
- [28] Dong Huk Park, Samaneh Azadi, Xihui Liu, Trevor Darrell, and Anna Rohrbach. Benchmark for compositional text-to-image synthesis. In *Thirty-fifth Conference on Neural Information Processing Systems Datasets and Benchmarks Track (Round 1)*, 2021. 7
- [29] Peng Qi, Yuhao Zhang, Yuhui Zhang, Jason Bolton, and Christopher D Manning. Stanza: A python natural language processing toolkit for many human languages. *arXiv preprint arXiv:2003.07082*, 2020. 1
- [30] Alec Radford, Jong Wook Kim, Chris Hallacy, Aditya Ramesh, Gabriel Goh, Sandhini Agarwal, Girish Sastry, Amanda Askell, Pamela Mishkin, Jack Clark, Gretchen Krueger, and Ilya Sutskever. Learning transferable visual models from natural language supervision, 2021. 3, 1
- [31] Alec Radford, Jong Wook Kim, Chris Hallacy, Aditya Ramesh, Gabriel Goh, Sandhini Agarwal, Girish Sastry, Amanda Askell, Pamela Mishkin, Jack Clark, et al. Learning transferable visual models from natural language supervision. In *International conference on machine learning*, pages 8748–8763. PMLR, 2021. 7
- [32] Colin Raffel, Noam Shazeer, Adam Roberts, Katherine Lee, Sharan Narang, Michael Matena, Yanqi Zhou, Wei Li, and Peter J Liu. Exploring the limits of transfer learning with a unified text-to-text transformer. *The Journal of Machine Learning Research*, 21(1):5485–5551, 2020. 2

- [33] Aditya Ramesh, Mikhail Pavlov, Gabriel Goh, Scott Gray, Chelsea Voss, Alec Radford, Mark Chen, and Ilya Sutskever. Zero-shot text-to-image generation. In *International Conference on Machine Learning*, pages 8821–8831. PMLR, 2021. 1, 2
- [34] Aditya Ramesh, Prafulla Dhariwal, Alex Nichol, Casey Chu, and Mark Chen. Hierarchical text-conditional image generation with clip latents. *arXiv preprint arXiv:2204.06125*, 2022. 2
- [35] Robin Rombach, Andreas Blattmann, Dominik Lorenz, Patrick Esser, and Björn Ommer. High-resolution image synthesis with latent diffusion models. In *Proceedings of the IEEE/CVF conference on computer vision and pattern recognition*, pages 10684–10695, 2022. 1, 2, 3, 5
- [36] Chitwan Saharia, William Chan, Saurabh Saxena, Lala Li, Jay Whang, Emily L Denton, Kamyar Ghasemipour, Raphael Gontijo Lopes, Burcu Karagol Ayan, Tim Salimans, et al. Photorealistic text-to-image diffusion models with deep language understanding. *Advances in Neural Information Processing Systems*, 35:36479–36494, 2022. 1, 2, 7
- [37] Jascha Sohl-Dickstein, Eric Weiss, Niru Maheswaranathan, and Surya Ganguli. Deep unsupervised learning using nonequilibrium thermodynamics. In *International conference on machine learning*, pages 2256–2265. PMLR, 2015. 3
- [38] Yang Song and Stefano Ermon. Generative modeling by estimating gradients of the data distribution. *Advances in neural information processing systems*, 32, 2019. 4
- [39] Ming Tao, Hao Tang, Fei Wu, Xiao-Yuan Jing, Bing-Kun Bao, and Changsheng Xu. Df-gan: A simple and effective baseline for text-to-image synthesis. In *Proceedings of the IEEE/CVF Conference on Computer Vision and Pattern Recognition*, pages 16515–16525, 2022. 2
- [40] Dani Valevski, Matan Kalman, Yossi Matias, and Yaniv Leviathan. Unitune: Text-driven image editing by fine tuning an image generation model on a single image. *arXiv preprint arXiv:2210.09477*, 2022. 3
- [41] Pascal Vincent. A connection between score matching and denoising autoencoders. *Neural computation*, 23(7):1661–1674, 2011. 4
- [42] Andrey Voynov, Kfir Aberman, and Daniel Cohen-Or. Sketch-guided text-to-image diffusion models. In *ACM SIGGRAPH 2023 Conference Proceedings*, pages 1–11, 2023. 3, 2
- [43] Ekaterina Vylomova, Laura Rimell, Trevor Cohn, and Timothy Baldwin. Take and took, gaggle and goose, book and read: Evaluating the utility of vector differences for lexical relation learning. *arXiv preprint arXiv:1509.01692*, 2015. 2
- [44] Tengfei Wang, Ting Zhang, Bo Zhang, Hao Ouyang, Dong Chen, Qifeng Chen, and Fang Wen. Pretraining is all you need for image-to-image translation. *arXiv preprint arXiv:2205.12952*, 2022. 3
- [45] Zijie J Wang, Evan Montoya, David Munechika, Haoyang Yang, Benjamin Hoover, and Duen Horng Chau. Diffusiondb: A large-scale prompt gallery dataset for text-to-image generative models. *arXiv preprint arXiv:2210.14896*, 2022. 2
- [46] Qiucheng Wu, Yujian Liu, Handong Zhao, Ajinkya Kale, Trung Bui, Tong Yu, Zhe Lin, Yang Zhang, and Shiyu Chang. Uncovering the disentanglement capability in text-to-image diffusion models. In *Proceedings of the IEEE/CVF Conference on Computer Vision and Pattern Recognition*, pages 1900–1910, 2023. 2, 3
- [47] Tao Xu, Pengchuan Zhang, Qiuyuan Huang, Han Zhang, Zhe Gan, Xiaolei Huang, and Xiaodong He. Attngan: Fine-grained text to image generation with attentional generative adversarial networks. In *Proceedings of the IEEE conference on computer vision and pattern recognition*, pages 1316–1324, 2018. 2
- [48] Hui Ye, Xiulong Yang, Martin Takac, Rajshekhar Sunderraman, and Shihao Ji. Improving text-to-image synthesis using contrastive learning. *arXiv preprint arXiv:2107.02423*, 2021. 2
- [49] Jiahui Yu, Yuanzhong Xu, Jing Yu Koh, Thang Luong, Gungjan Baid, Zirui Wang, Vijay Vasudevan, Alexander Ku, Yinfei Yang, Burcu Karagol Ayan, et al. Scaling autoregressive models for content-rich text-to-image generation. *arXiv preprint arXiv:2206.10789*, 2022. 2
- [50] Han Zhang, Jing Yu Koh, Jason Baldridge, Honglak Lee, and Yinfei Yang. Cross-modal contrastive learning for text-to-image generation. In *Proceedings of the IEEE/CVF conference on computer vision and pattern recognition*, pages 833–842, 2021. 2
- [51] Lvmin Zhang, Anyi Rao, and Maneesh Agrawala. Adding conditional control to text-to-image diffusion models. In *Proceedings of the IEEE/CVF International Conference on Computer Vision*, pages 3836–3847, 2023. 3
- [52] Minfeng Zhu, Pingbo Pan, Wei Chen, and Yi Yang. Dm-gan: Dynamic memory generative adversarial networks for text-to-image synthesis. In *Proceedings of the IEEE/CVF conference on computer vision and pattern recognition*, pages 5802–5810, 2019. 2

Semantic Guidance Tuning for Text-To-Image Diffusion Models

Supplementary Material

	Inference Time (s)
Stable Diffusion	6.7
Composable Diffusion	17.4
Structure Diffusion	18.5
Attend-and-Excite	20.2
Ours	18.3

Table 3. Average inference time on Dense MS-COCO Dataset [17].

6. Additional Details.

6.1. Implementation

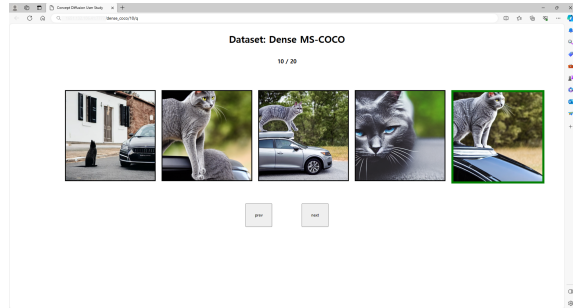
In our experiments, we utilize the official Stable Diffusion v1.4 text-to-image model, integrated with the pre-trained text encoder CLIP ViT-L/14 [30]. We consistently apply a fixed guidance scale w_g of 7.5 across all experiments. To ensure consistency in our results, we use a fixed random seed to generate the same initial Gaussian map for each experiment and employ 50 timesteps with PLMS sampling [22] for the diffusion process. For parsing and identifying subject concepts from the prompts, we use the Stanza Library [29]. Specifically, we extract noun phrases from the lowest level of the constituency tree as our subject concepts. We set the concept guidance scale w_c to 7.5 and the threshold η is set to $1/(n+1)$, where n is the number of subject concepts. The concept guidance is applied in every timestep t .

6.2. Inference Time

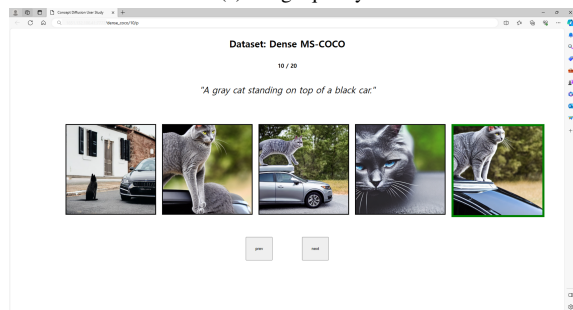
To assess the efficiency of the baseline methods in terms of inference time, we conduct an evaluation. We generate 10 images for each method using complex prompts from Dense MS-COCO dataset [17]. The average inference time for each method is then calculated, with all tests conducted on a single RTX 3090 GPU. The results is in Tab. 3. Composable Diffusion, Structure Diffusion, and Concept Diffusion approximately triple the inference time. This increase is attributed to their reliance on running multiple diffusion processes. For Attend-and-Excite, despite utilizing only a single diffusion process, the method prolongs the inference time due to its iterative gradient-based optimization approach.

6.3. User Study

We conduct a user study involving 40 participants to assess the effectiveness of our method. In each task, participants are presented with a set of images that are generated using the same prompt and random seeds. The study is structured



(a) Image quality



(b) Semantic alignment

Figure 8. User study interface



(a) w/o abstract concept



(b) Concept Diffusion

Figure 9. **Ablation study.** We show example results on the prompt “a blue backpack and a brown sheep”, when abstract concept is ablated from our method. Note that without abstract concept, subjects tend to fuse.

in two phases. Initially, participants are asked to select the image they consider to be of the highest quality, without knowledge of the prompt. Following this, the prompt is revealed, and they are then asked to choose the image that they believe best followed the prompt. To ensure unbiased responses, the order in which the images are presented is randomized in every round. Fig. 8 shows the interface used for user study.

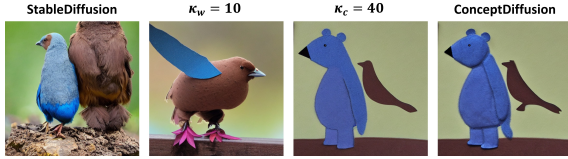


Figure 10. **Ablation study.** Images generated using the prompt “a brown bird and a blue bear” when a warm-up period and a cool-down period is used.

7. Ablation study

7.1. Abstract Concept

In this subsection, we validate the use of abstract concept along with subject concept. As discussed, steering the guidance direction towards the abstract concept helps prevent the fusion of subjects in the generated image. This is illustrated in Fig. 9, where we present images generated with and without the inclusion of an abstract concept in concept guidance for the prompt “a blue backpack and a brown sheep”. The comparison distinctly shows that when the model relies solely on subject concepts, it successfully synthesizes images containing both a sheep and a backpack. However, in these images, the subjects are merged together, leading to an unnatural fusion, such as a sheep with a head resembling a blue backpack. In contrast, the inclusion of the abstract concept results in a significant improvement. When the abstract concept is used, the model not only generates all the subjects but also clearly separates them. The resulting image distinctly features both the sheep and the backpack as separate entities, effectively illustrating the advantages of incorporating an abstract concept.

7.2. Concept Guidance Schedule

Throughout the experiments, we use concept guidance at every timestep t when the similarity between the prompt score and each concept score is below the threshold η . Recent works have suggested that the spatial location of each subject is determined in the early denoising steps [9, 42] and after most of the denoising has occurred, the diffusion model’s self-attention layers play a large role, making the guidance less impactful [2]. Therefore, in this subsection, we closely examine when to apply concept guidance effectively. Specifically, we set a warm-up periods κ_w and a cool-down periods κ_c . The concept guidance scale w_c is set to 0 when $\kappa_w < t$ or $t > \kappa_c$.

Fig. 10 illustrates the impact of these periods on image synthesis using the prompt “a brown bird and a blue bear”. When a warm-up period is used, the model fails to fully synthesize all subjects. For instance, while the color of the bird changes from blue to brown, the bear is not present in the image. Conversely, when a cool-down period is used, we observe a degradation in image quality, such as the bird

appearing with missing legs. Accordingly, our full Concept Diffusion method does not employ either the warm-up or cool-down period parameters. We determine that omitting these periods allows more consistent and effective application of concept guidance throughout the entire process of image generation.

8. Additional Comparison

Here in Fig. 11 and Fig. 12, we present additional qualitative comparison with baseline methods.

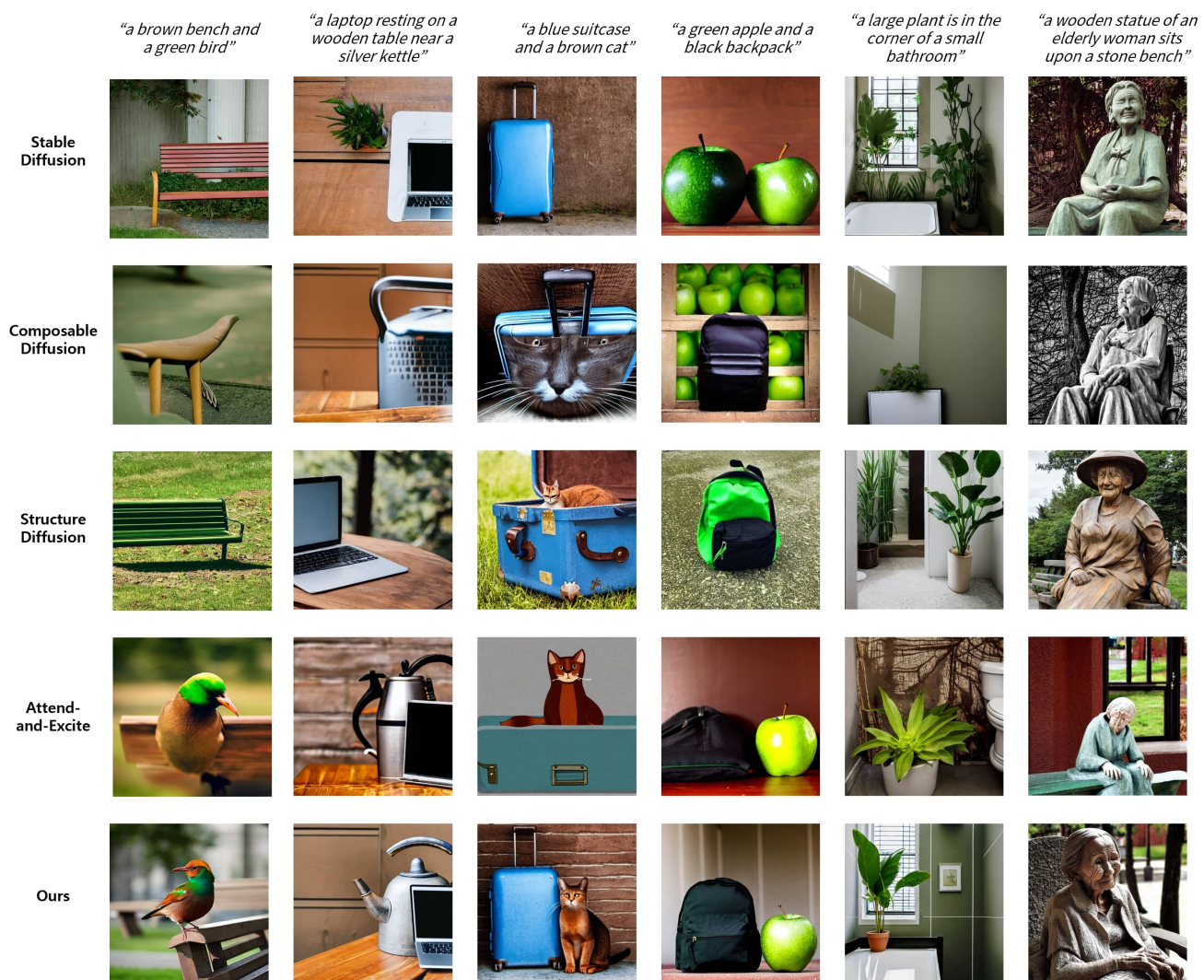


Figure 11. More results on CC-500 Dataset [7].

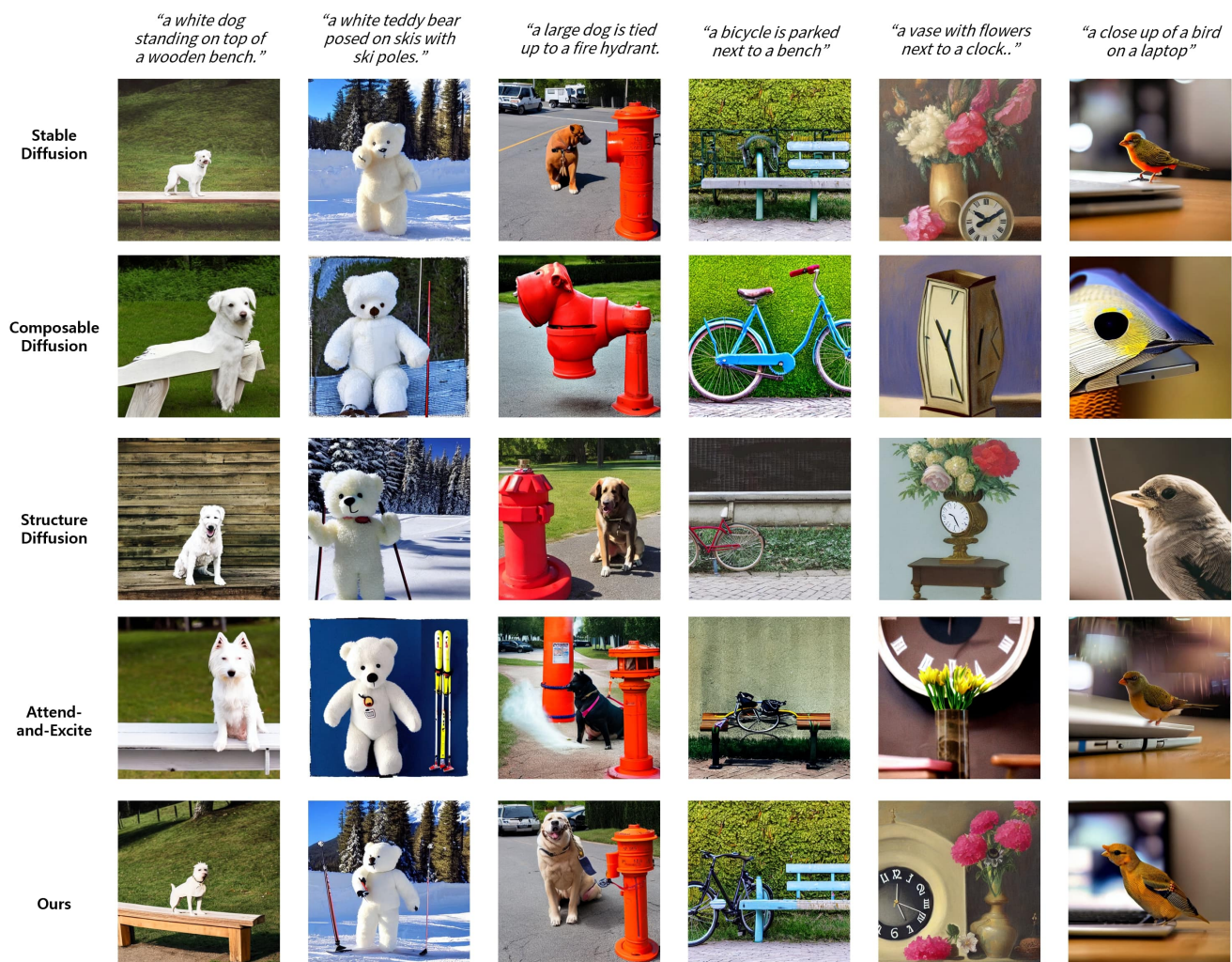


Figure 12. More results on Dense MS-COCO Dataset [17].